EXHIBIT 14

SILICON PROCESSING FOR THE VLSI ERA

VOLUME 1:

PROCESS TECHNOLOGY

STANLEY WOLF Ph.D.
Professor, Department of Electrical Engineering
California State University, Long Beach
Long Beach, California
and
Instructor, Engineering Extension, University of California, Irvine

RICHARD N. TAUBER Ph.D.
Manager of VLSI Fabrication
TRW - Microelectronics Center
Redondo Beach, California
and
Instructor, Engineering Extension, University of California, Irvine

LATTICE PRESS
Sunset Beach, California

DISCLAIMER

This publication is based on sources and information believed to be reliable, but the authors and Lattice Press disclaim any warranty or liability based on or relating to the contents of this publication.

Published by:

Lattice Press
Post Office Box 340
Sunset Beach, California 90742, U.S.A.

Cover design by Roy Montibon and Donald Strout, Visionary Art Resources, Inc., Santa Ana, CA.

Library of Congress Cataloging in Publication Data
Wolf, Stanley and Tauber, Richard N.

Silicon Processing for the VLSI Era
Volume 1 : Process Technology

Includes Index
1. Integrated circuits-Very large scale integration. 2. Silicon. I. Title

86-081923

ISBN 0-961672-3-7

11 12 13 14 15

PRINTED IN THE UNITED STATES OF AMERICA

models, several references are given at the end of the chapter. Some are comprehensive surveys[1,2], while others are papers in which the models were originally published (and which thus discuss more fully the assumptions underlying the model, and details of the derivations and associated calculations[3,4,5]).

Definitions Associated with Ion Implantation Profiles

As energetic ions penetrate a solid target material, they lose energy due to collisions with atomic nuclei and electrons in the target, and eventually come to rest. The total distance that an ion travels in the target before coming to rest is termed the *range*, R. As a result of the collisions between the ions and the target material nuclei, this trajectory is not a straight line (and in fact, the value of the total distance traveled is not even the quantity that is of highest interest). What is of greater interest than R is the projection of this range on the direction parallel with the incident beam, since this represents the penetration depth of the implanted ions along the implantation direction. This quantity is called the *projected range*, R_p (Fig. 2a). As the number of collisions (and the energy lost per collision experienced by the penetrating ion) are random variables, ions having the same initial energy and mass will end up spatially distributed in the target. An average ion will stop at a depth below the surface given by R_p. Some ions, however, undergo fewer scattering events than the average, and come to rest more deeply into the target. Others suffer more collisions, and come to rest closer to the surface than R_p. As a result, when large numbers of ions are implanted, R_p corresponds to the depth at which most ions stop, and this is the distance at which the profile has maximum value. The statistical fluctuation along the direction of the projected range is given by the quantity known as the *projected straggle*, ΔR_p (Fig. 2b).

The ions are also scattered to some degree along the direction perpendicular to the incident direction, and the statistical fluctuation along this direction is called the *projected lateral straggle*, $\Delta R_\perp$ (Fig. 2b). Information about the lateral straggle is important because it describes the extent

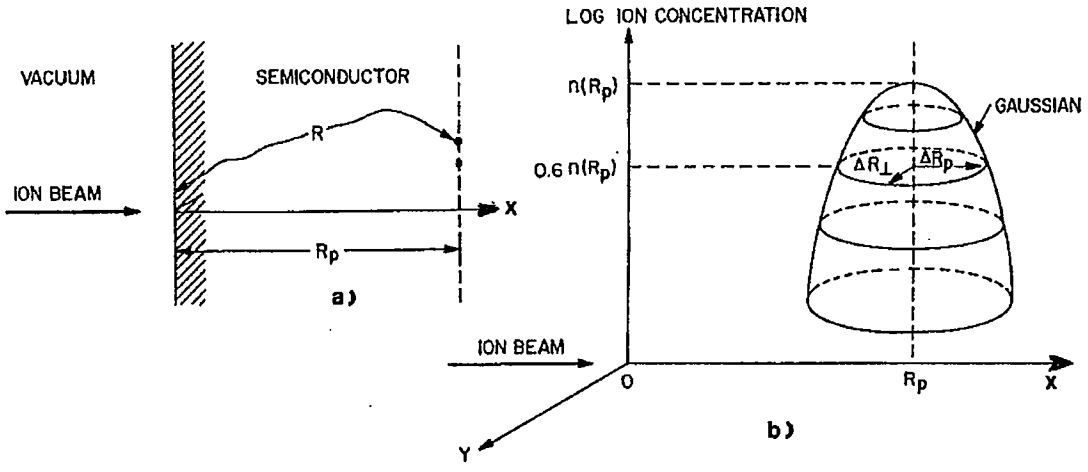

Fig. 2 a) Schematic of the ion range, R, and projected range, R_p. b) Two-dimensional distribution of the implanted atoms. From S.M. Sze, *Semiconductor Devices, Physics and Technology*, Copyright © 1985 John Wiley & Sons. Reprinted with permission of John Wiley & Sons.

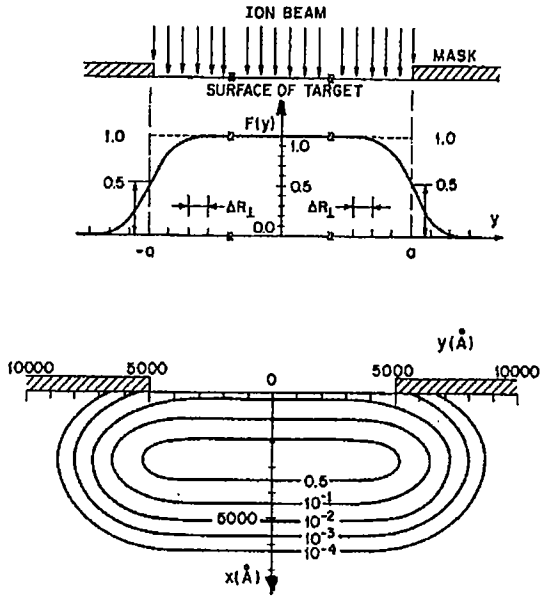

Fig. 3 Illustration of lateral profiles. (a) Ion concentration along the lateral direction (y) for a gate mask with $a >> \Delta R_{\perp}$ and infinite extension in the x-direction. (b) Contours of equal-ion concentrations for 70 keV B^+ (R_p = 2710Å, ΔR_p = 824Å, and $\Delta R_{\perp}$ = 1006Å) incident into silicon through a 1 μm slit[6]. Reprinted with permission of Japanese Journal of Applied Physics.

of lateral penetration of ions under the edges of implant masks. Such lateral penetration may represent a limiting dimension in some integrated circuit device structures. In general, values of ΔR_p and $\Delta R_{\perp}$ are within ±20% of one another. Figure 3a shows an opening in a "thick" mask material, and resultant ion concentrations in the lateral direction in the target. It is seen that lateral straggle effects cause implanted ions to be distributed under edges of the mask. In Fig. 3b contours of equal-ion concentration for 70-keV B atoms implanted into a 1-μm slit are shown[6].

Theory of Ion Stopping

As an ion moves through a solid target, it transfers energy by collisions with the target nuclei (*nuclear collisions*) and by Coulombic interaction with the electrons in the target material. In the latter mechanism, the energy transferred to the electrons can lead to exciting the electrons to higher energy levels (*excitation*), or to the ejection of electrons from their atomic orbits (*ionization*). The energy loss due to such target interactions gradually slows the ion, eventually bringing it to a stop. If the energy of the ion at any point along its trajectory in the target is given by E, the process of *energy loss through nuclear collisions* can be characterized by an *energy loss per unit length due to nuclear stopping*, $S_n(E)$, and *energy loss from interactions with target electrons* by an *energy loss per unit length due to electronic stopping*, $S_e(E)$. The total rate of energy loss $(dE/dx)_{total}$ is given by the sum of these stopping mechanisms:

$$\left[\frac{dE}{dx}\right]_{total} = S_n(E) + S_e(E) \qquad (2)$$

If the total distance that the ion travels before coming to a complete stop is given by R, then:

$$R = \int_0^{E_o} \frac{dE}{(-dE/dR)} \qquad (3)$$

where E_o is the initial incident ion energy.

The *nuclear stopping process* can be visualized with the aid of the extreme simplification that treats the event as a collision between two hard spheres (Fig. 4), or by a more correct approximation that assumes that the scattering is described by a Coulombic force-at-a-distance interaction. In the latter description, an appropriate atomic scattering potential, V(r), must be determined. The most successful model for predicting implantation profiles based on the ion stopping approach is the so called *LSS model*, which is discussed in further detail in the following section. The LSS model utilizes a modified Thomas-Fermi screened potential for V(r). Calculations based on this model show that nuclear stopping increases linearly in effectiveness at low energies, reaches a maximum at some intermediate energy, and decreases at higher energies, because at high velocity, ions move past target nuclei too quickly to efficiently transfer energy to them. Values of $S_n(E)$ for boron, phosphorus, and arsenic are shown in Fig. 5. It is important to note that $S_n(E)$ increases with the mass of the implanted ion, and thus heavy ions such as As will transfer much more of their energy through nuclear collisions than will B atoms.

The *electronic stopping process* can be considered as similar to the stopping of a projectile in a viscous medium, and the stopping magnitude can be approximated to be proportional to the square root of the ion velocity:

$$S_e(E) = k_e (E)^{1/2} \qquad (4)$$

where k_e is a constant that depends weakly on the ion and target atomic masses and numbers. Figure 5 also shows $S_e(E)$ for B, P, and As. As can be seen in Fig. 5 the crossover energy at which electronic stopping becomes more effective than nuclear stopping is higher for heavier ions. For example, for boron $S_e(E)$ is the predominant energy loss mechanism down to ~10 keV, while for P and As, the energy loss due to nuclear stopping predominates for energies up to 130 keV and 700 keV, respectively.

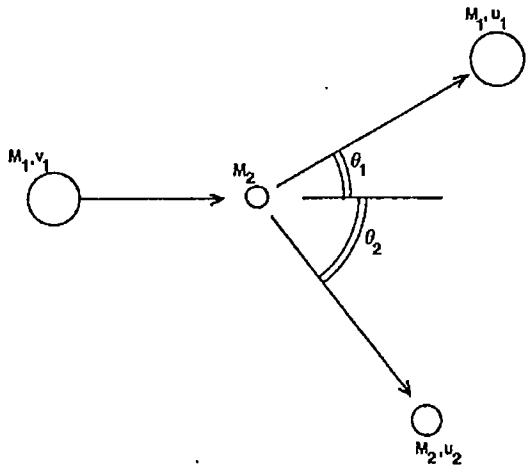

Fig. 4 Collision between two particles treated as if they are hard spheres.

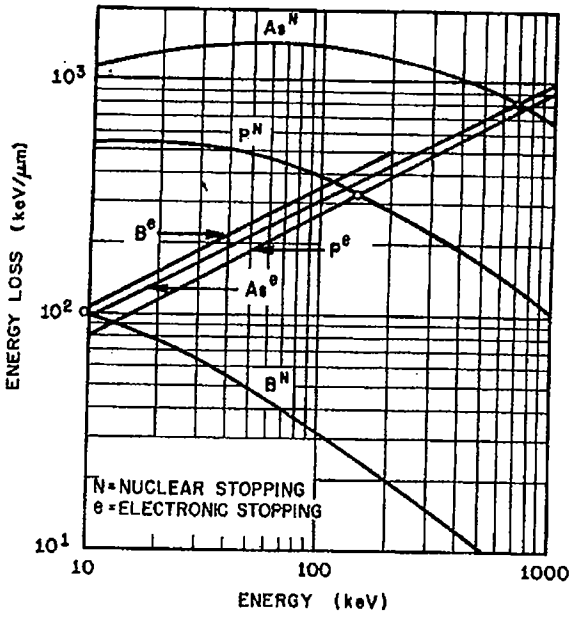

Fig. 5 Calculated values of dE/dx for As, P, and B at various energies. The nuclear (N) and electronic (e) components are shown. Note the points (o) at which nuclear and electronic stopping are equal. (After Smith, Ref. 7, redrawn by Seidel in Ref. 63, Copyright, 1983, Bell Telephone Laboratories, Incorporated, reprinted by permission.)

Models for Implantation Profiles in Amorphous Solids

The range-energy relation given by Eq. 2 was reformulated by Lindhard, Scharff, and Schiott (LSS) for implantation into amorphous material in terms of the reduced parameters, ε and ρ, as:

$$\frac{d\varepsilon}{d\rho} = \left(\frac{d\varepsilon}{d\rho}\right)_n + k_\varepsilon (\varepsilon)^{1/2} \qquad (5)$$

where ρ and ε are dimensionless variables related to the range, R, and incident energy, E_o, by:

$$\rho = \frac{(R\,N\,M_1\,M_2\,4\pi a^2)}{(M_1 + M_2)} \qquad (5a)$$

and;

$$\varepsilon = \frac{E_o\,a\,M_2}{[Z_1 Z_2 q^2 (M_1 + M_2)]} \qquad (5b)$$

where: M_1 and M_2 are the mass of the incident ions and target atoms, respectively; N is the number of atoms per unit volume; a is the screening length, equal to $0.88a_o/(Z_1^{1/3} + Z_2^{2/3})^{1/2}$ and a_o is the Bohr radius; and Z_1 and Z_2 are the atomic numbers of the ion and target.

LSS used a modified Thomas-Fermi screened potential to calculate the energy loss due to nuclear stopping, together with the assumption that the energy loss due to electronic stopping is given by Eq. 4 (Fig. 6). Using this approach, they calculated values of ρ for different values of ε. (Note that these calculations are quite complex, but can be found in the classic paper by

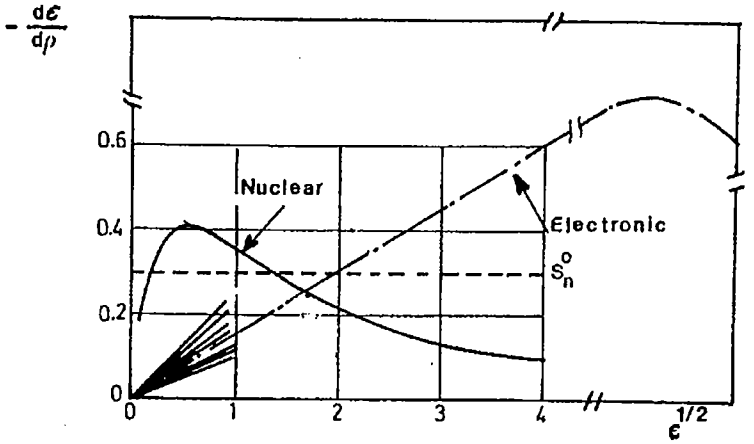

Fig. 6 (a) Nuclear stopping power for Thomas-Fermi potential (solid line) and electronic stopping power (dash-dot line) for k = 0.15 in terms of the reduced variables ε and ρ, based on LSS theory[3]. (b) Representation of as-implanted impurity profiles by joined half-Gaussian distributions.

LSS[3].) The value of ρ was then converted to R (using Eq. 5a), and finally a value for R_p was obtained from the approximate expression[8]:

$$R_p \cong \frac{R}{1 + \left[\frac{M_2}{3 M_1}\right]} \qquad (6)$$

LSS assumed that the distribution of the implanted ions in amorphous materials could be described by a symmetrical Gaussian curve (see Chap. 18, Fig. 2). If this assumption is valid, then the implanted ion concentration, n, as a function of depth, x, can be described by:

$$n(x) = \frac{\phi}{\sqrt{2\pi}\,\Delta R_p} \exp\left[\frac{-(x - R_p)^2}{2\Delta R_p^2}\right] \qquad (7)$$

where: ϕ is the dose (in number of implanted ions /cm^2), and ΔR_p is the standard deviation of the Gaussian distribution (or *projected straggle* of the distribution in the direction of incidence of the beam). The value of ΔR_p is calculated in terms of R_p and the mass of the implanted ions M_1 and the target atoms M_2, by the approximate expression[8]:

$$\Delta R_p \cong \frac{2 R_p}{3}\left[\frac{\sqrt{M_1 M_2}}{M_1 + M_2}\right] \qquad (8)$$

The concentration is maximum at R_p, and Eq. 7 at $x = R_p$ reduces to:

$$n(x = R_p) = \frac{\phi}{\sqrt{2\pi}\,\Delta R_p} \cong \frac{0.4\,\phi}{\Delta R_p} \qquad (9)$$

The assumption by LSS that the distribution of implanted atoms in amorphous materials is well approximated by a Gaussian curve is not completely correct, but is nevertheless very useful as a first order description. Indeed, the fit to experiment is almost always good for all implantations near the peak. For example, the peak value predicted by Eq. 9 is generally within

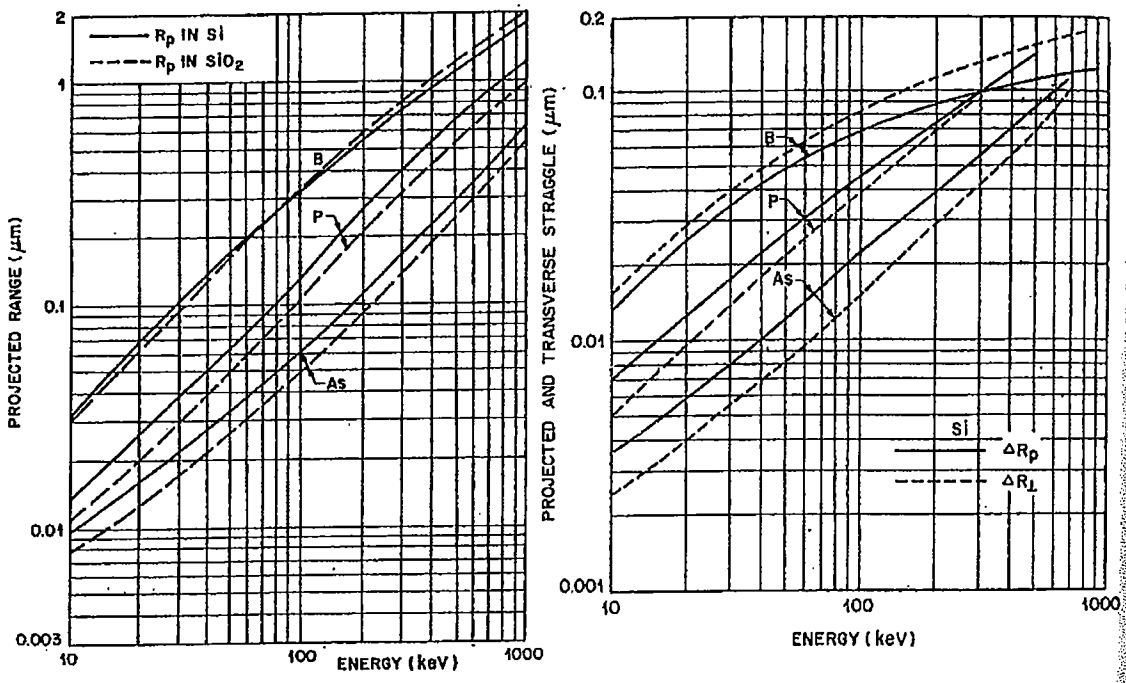

Fig. 7 (Left) Projected range for B, P, and As in Si and SiO_2 at various energies. The results pertain to amorphous silicon targets and thermal SiO_2 (2.27 g /cm^3). After Smith, Ref. 7, redrawn by Seidel in Ref. 63, Copyright, 1983, Bell Telephone Laboratories, Incorporated, reprinted by permission. **Fig. 8 (Right)** Calculated ion projected straggle ΔR_p, and ion lateral straggle $\Delta R_\perp$ for As, P, and B ions in silicon. After Smith, Ref. 7, redrawn by Seidel in Ref. 63, Copyright, 1983, Bell Telephone Laboratories, Incorporated, reprinted by permission.

1% of the measured value, except for very shallow [low energy] implants]. On the other hand, significant asymmetries begin to appear in experimental implant profiles in amorphous targets once the concentration levels drop by a factor of 10 below the peak value (and which are not taken into account by a symmetrical Gaussian approximation). Therefore, various distribution curves with a higher number of moments than a Gaussian (which can be described with only two moments, R_p and ΔR_p), have been examined for their ability to fit the experimental implant profiles (Fig. 1). In addition, LSS theory and the Gaussian curve fail to account for several effects that occur when implants are made into *single-crystal* material. Thus, modifications or even other analytical models must be used to obtain a good fit to data obtained in such situations.

Nevertheless, in practice the Gaussian distribution is still commonly used to provide quick estimates of doping distributions into amorphous and single-crystal targets. The higher moment distributions (or alternate models) are subsequently utilized to fine tune the dose or energy to obtain better results. Several workers have calculated R_p and ΔR_p values, using LSS theory to perform the calculations, for many of the elements that are commonly implanted into Si and SiO_2. Figure 7 is an example of such data for B, P, and As into silicon. Values for projected lateral straggle, $\Delta R_\perp$, have also been compiled, and are given in Fig. 8 (together with ΔR_p).

Example: A 150 mm wafer is to be implanted with 100 keV boron atoms to a dose of 5×10^{14} ions /cm^2. 1) Determine the projected range, projected straggle, and peak concentration using Figs. 7 and 8. 2) If the implantation time is 1 min, calculate the required ion beam current.

Solution: 1) From Figs. 7 and 8, it is found that the *projected range* and *projected straggle* are 0.32 μm and 0.07 μm, respectively. The peak concentration, $N(x = R_p)$, can be calculated from Eq. 9, or:

$$N(x = Rp) = \frac{0.4\,\phi}{\Delta R_p} = \frac{0.4\,(5\times10^{14})}{(0.07\times10^{-4}\ \text{cm})} = 2.8\times10^{19}\ \text{ions/cm}^3$$

2) To find the beam current, first calculate the total number of implanted ions (Q = dose * wafer area:

$$Q = (5\times10^{14}\ \text{ions/cm}^2)*[\,\pi\,(15/2)^2\,] = 8.8\times10^{16}\ \text{ions}$$

Then, the required scanned beam current is determined by dividing the total charge, qQ, by the time of implantation:

$$I = (qQ/t) = [(1.6\times10^{-19}\ \text{C})\ (8.8\times10^{16})]/60\ \text{sec} = 0.23\ \text{mA}.$$

Higher Moment Distributions for Implant Profiles in Amorphous Material

As noted earlier, even when implanting into amorphous material, the experimental profiles exhibit some asymmetry, or *skewness*. This is not surprising if one considers the forward momentum of the ions. That is, when relatively light atoms make collisions with target atoms (e.g. B in Si), they experience a significant degree of backscattering. Hence more will come to rest at a distance closer to the surface than R_p (causing the concentration near the surface to be higher). On the other hand, heavier atoms will undergo little backscattering, and the concentration on the deep side will be higher. Thus, even if a Gaussian distribution is used to approximate the implantatation profile, such non-Gaussian effects on the behavior of devices can be anticipated. That is, when boron is utilized to implant deep p-wells (in CMOS technology), higher doping close to the surface is expected (than predicted by a Gaussian distribution). On the other hand, the skewness in arsenic implants will produce deeper junctions than predicted when implanting n^+ source /drain, or emitter regions with arsenic.

To theoretically account for the skewness found in measured profiles, probability

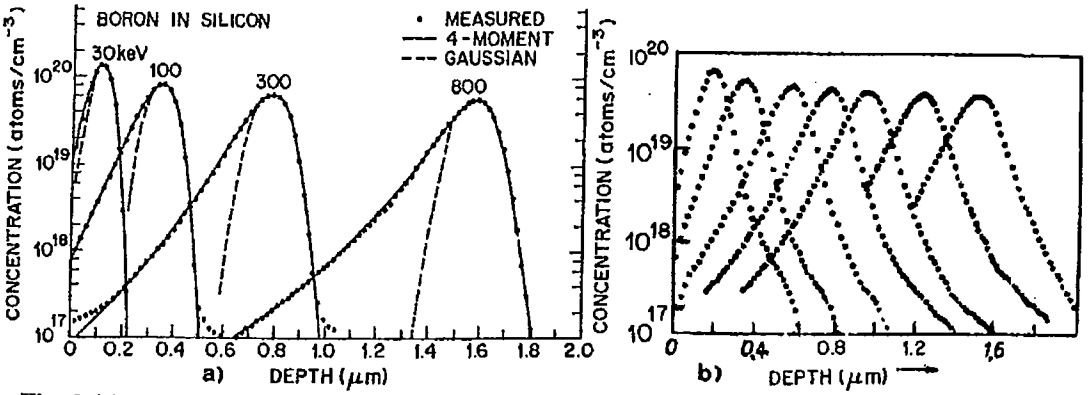

Fig. 9 (a) Boron implanted atom distributions, showing 1) measured data points, 2) four-moment (Pearson-IV) curves, and 3) symmetric Gaussian curves. The boron was implanted into *amorphous silicon* without annealing. (b) Depth distributions of boron implanted in *crystalline silicon* in a <763> direction - a dense crystallographic direction at various energies. *Tails* occur because of channeling effect[5]. Reprinted with permission of Philips Research Reports.